Journal of Inflammation Research

Dovepress
open access to scientific and medical research

Open Access Full Text Article

ORIGINAL RESEARCH

Inflammation-Related Gene ADH1A Regulates the Polarization of Macrophage M1 and Influences the Malignant Progression of Gastric Cancer

Jun Ma[1], Yongkang Shi[1], Qiliang Lu[1], Dongsheng Huang[2]

[1]General Surgery, Cancer Center, Department of Gastrointestinal and Pancreatic Surgery, Zhejiang Provincial People's Hospital, Affiliated People's Hospital, Hangzhou Medical College, Hangzhou, Zhejiang, People's Republic of China; [2]Key Laboratory of Tumor Molecular Diagnosis and Individualized Medicine of Zhejiang Province, Zhejiang Provincial People's Hospital, Affiliated People's Hospital, Hangzhou Medical College, Hangzhou, Zhejiang, People's Republic of China

Correspondence: Dongsheng Huang, Key Laboratory of Tumor Molecular Diagnosis and Individualized Medicine of Zhejiang Province, Zhejiang Provincial People's Hospital, Affiliated People's Hospital, Hangzhou Medical College, No. 158 Shangtang Road, Gongshu District, Hangzhou, Zhejiang, 310014, People's Republic of China, Tel/Fax +86-571-88927749, Email dshuang126@163.com

Background: Gastric cancer (GC) is a malignant tumor originating from the gastric mucosa epithelium, and there is a low survival rate of GC patients after treatment, with a poor prognostic outcome. The inflammatory response within the tumor microenvironment plays an important role in GC progression.

Methods: We downloaded GC-related datasets and inflammation-related genes from GEO, TCGA and MSigDB databases, performed differential analysis, protein-protein interaction analysis, immunoinfiltration analysis and Lasso analysis to screen inflammation-related hub genes affecting GC progression, and carried out qRT-PCR for validation. In order to explore the role of ADH1A, we constructed overexpressed plasmids, treated GC cells with cGMP/PKG pathway agonist 8-Br-cGMP, and tested cell functions with CCK8, EdU, Transwell, scratch assay and other experiments. On this basis, GC cells were co-cultured with monocyte THP-1 to explore the effect of ADH1A on the polarization of macrophages.

Results: ADH1A was significantly decreased in GC cells, and its expression trend was consistent with the results of bioinformatics analysis. Therefore, we chose ADH1A for subsequent functional validation. Overexpression of ADH1A in GC cells revealed ADH1A's role in inhibiting the activity, proliferation, migration and invasion of GC cells, promoting apoptosis and secretion of IL-6, IFN-γ, CCL5 and CSF2, and facilitating the transformation of macrophages to a pro-inflammatory M1 phenotype. ssGSEA results demonstrated the potential involvement of ADH1A in the cGMP/PKG signaling pathway, and significant changes in the expression of proteins related to the cGMP/PKG signaling pathway. The use of the cGMP/PKG signaling pathway agonist 8-Br-cGMP in ADH1A-overexpressing GC cells substantiated ADH1A's capacity to inhibit the cGMP/PKG signaling pathway, thereby suppressing the malignant progression of GC and promoting the transformation of macrophages to a pro-inflammatory M1 phenotype.

Conclusion: ADH1A is able to influence the malignant progression of GC and the transformation of macrophages to the pro-inflammatory M1 phenotype through the cGMP/PKG signaling pathway.

Keywords: gastric cancer, inflammation, immune infiltration analysis, ADH1A, cGMP/PKG signaling pathway

Introduction

Gastric cancer (GC) is the world's fifth most common malignant tumor, posing a significant global health concern. Diagnosed typically at an advanced stage, patients with GC have a high mortality rate, which ranks GC as the third leading cause of cancer-related deaths,[1] with an extremely low 5-year survival rate.[2] *Helicobacter pylori* infection is the main cause and one of the major risk factors of GC,[3] despite declining infection rates due to economic development and improved living standards. Unhealthy dietary habits, including high salt, fat and cholesterol intake, contribute to elevated GC risk.[4] While familial aggregation is observed in GC cases, only 1–3% demonstrate autosomal dominant inheritance.[5] In addition, hormonal factors, particularly estrogen, contribute to the male predominance in GC cases.[6] Screening

Received: 30 November 2023
Accepted: 15 June 2024
Published: 12 July 2024

© 2024 Ma et al. This work is published and licensed by Dove Medical Press Limited. The full terms of this license are available at https://www.dovepress.com/terms.php and incorporate the Creative Commons Attribution – Non Commercial (unported, v3.0) License (http://creativecommons.org/licenses/by-nc/3.0/). By accessing the work you hereby accept the Terms. Non-commercial uses of the work are permitted without any further permission from Dove Medical Press Limited, provided the work is properly attributed. For permission for commercial use of this work, please see paragraphs 4.2 and 5 of our Terms (https://www.dovepress.com/terms.php).

initiatives, notably in Japan and South Korea, have significantly reduced cancer-related mortality.[1] Therefore, exploring disease markers for GC is crucial for its early intervention and progression assessment, which in turn prevent its potential malignant progression and metastasis.

Inflammation is considered a critical cancer marker, and it is beneficial for fostering a conducive environment for tumor cell growth, invasion and metastasis through the secretion of various inflammatory mediators. During inflammation-induced tumorigenesis, the pro-tumor immune effect outweighs the anti-tumor immune effect in the tumor microenvironment. Therefore, immunotherapy has emerged as a new targeted therapy for the treatment of advanced or metastatic GC. Approved immune checkpoint inhibitors (ICIs), including Nivolumab, Pembrolizumab and Toripalimab, target immune checkpoints (ICs) in immune cells to eliminate the inhibition of T cells by tumor cells, thereby promoting the body's immune response and enhancing the anti-tumor effects.[2] However, clinical use of ICIs in GC faces challenges, including low response rates, high drug resistance, and significant adverse reactions, which are related to the tumor immune microenvironment,[7] especially tumor-associated macrophages (TAMs). TAMs play an important role in promoting an inhibitory tumor immune microenvironment and immune evasion.[8] Targeting immunosuppressive immune cells and inflammatory mediators within the tumor microenvironment can improve the efficacy of anti-cancer therapies such as immunotherapy, radiotherapy, and chemotherapy. Therefore, investigating inflammation-related markers affecting GC progression and their potential connection with immune cells is essential. The identification of new and effective immunotherapy targets holds great significance for enhancing the efficacy and refining the clinical application of GC immunotherapy.

In this study, we used GC-related datasets downloaded from GEO and TCGA databases to screen inflammation-related target genes that affect GC progression. We aimed to investigate the potential targets to provide novel immunotherapy targets for the clinical treatment of GC.

Materials and Methods

Data Collection and Collation

We downloaded GC-related datasets from the TCGA database, retaining protein-encoding genes. Subsequently, 448 samples (410 tumor samples and 38 control samples) were included in the analysis. Additionally, the GC-related sequencing dataset GSE13911, comprising 69 samples (38 tumor samples and 31 control samples), were downloaded. From the Molecular Signatures Database (MSigDB), we extracted 200 inflammation-associated genes for further analysis (Supplementary Table 1).

Differential Analysis

The "edgeR" package (v 4.3.0) was used to conduct differential analysis of the samples, and then the "ggplot" package (v 3.4) to generate the volcano map and the "pheatmap" package to plot the heatmap.

Functional Enrichment Analysis

Functional enrichment analysis was conducted through gene set enrichment analysis (GSEA) in the "clusterProfiler" package, or the "clusterProfiler" package in conjunction with the "org.Hs.eg.db" package.

Protein-Protein Interaction (PPI) Analysis

We obtained the PPI data from the SRTING website (https://string-db.org/), and used the Cytoscape software to plot the interaction networks. Hub genes in the interactions were identified through MCC, MNC, DMNC, Degree, and EPC methods in the software.

Molecular Typing of GC

"ConsensusClusterPlus" was used to classify cancer samples by disease subtype, and then the "pROC" package (v 1.18) to plot the receiver operating characteristic curve (ROC).

Immune Infiltration Analysis

Immune infiltration analysis was conducted to clarify the composition of immune cells in the human microenvironment, and determine which immune cells play an important role in the occurrence and development of GC. CIBERSORT is a tool for deconvoluting the expression matrix of human immune cell subtypes based on the principle of linear support vector regression. In this study, we used the "CIBERSORT" package for immune infiltration analysis. Default parameters were used for performing analysis using the R package.

Machine Learning Algorithms

Least absolute shrinkage and selection operator (Lasso) is a data mining method commonly used in multiple linear regression. It adds a penalty function to continuously compress the coefficient, simplifying the model to avoid collinearity and overfitting. In this study, we used the "glmnet" (v 4.1) to perform Lasso regression analysis.

Correlation Analysis

Correlation analysis involves examining the relationship between two or more variable elements so as to measure their degree of correlation. In this study, we used the "ggcor" (v 0.98) to perform correlation analysis.

Cell Culture

Human GC cells AGS (Pricella, CL-0022), HGC-27 (Pricella, CL-0107), and SNU-16 (Beyotime, C6870), as well as human gastric epithelial cells GES-1 (Cobioer, CBP60512) were selected for analysis in this study. All cells were cultured at 37°C in an incubator containing 5% CO_2, with AGS cells cultured in Ham's F-12 (Pricella, PM150810) medium containing 10% fetal bovine serum (FBS, Pricella, 164210–50), HGC-27 cells cultured in RPMI-1640 (Pricella, PM150110) medium containing 20% FBS, SNU-16 cells cultured in RPMI 1640 medium containing 10% FBS, and GES-1 cells cultured in RPMI-1640 medium containing 10% FBS.

Macrophage Culture and Establishment of Co-Culture Systems

THP-1 cells (Pricella, CL-0233) were treated with PMA (Sigma, 100 ng/mL) for 24 h to obtain M0 macrophages. Simultaneously, supernatants of GC cells as well as associated cells were collected for culture-induced M0 macrophages.

Overexpression of ADH1A

GC cells were seeded in 12-well plates at a density of 1.2×10^5/well. After cell adhesion, adenovirus (Sangon Biotech) packaged with ADH1A was added and cultured for 24 h, followed by a 12-hour culture after a change of DMEM medium. Simultaneously, oe-NC was constructed as a control.

qRT-PCR

The Trizol method was applied for cellular RNA extraction. cDNA synthesis was carried out with the SuperScript™ VILO™ cDNA Synthesis Kit (Invitrogen, 11754050), and quantitative PCR was performed as per the SYBR Green dye method. The primers used in this experiment are shown in Table 1.

Western Blot (WB)

The total proteins were extracted from cells or tissues with a lysate containing 1% protease inhibitor, and then quantified by the BCA method (Beyotime, P0012S). Subsequent procedures included electrophoresis, membrane transfer, antibody incubation, and color development. Antibodies included ADH1A (Invitrogen, PA5-78730), PKG1 (proteintech, 21646-1-AP), PKG2 (proteintech, 55138-1-AP), pVASP (cell signaling technology, 3111), and VASP (cell signaling technology, 3132). GAPDH (#5174) was set as an internal reference protein.

Table 1 primers

Primer	Primer sequence
hsa-GFRA2-F	TGTCGCTGAACCTGTCTCCTC
hsa-GFRA2-R	CCTGCCTGCTTGTCTGTTTGG
hsa-ATP8A2-F	GCTATAAGAAGGCAGAGGATGAGATG
hsa-ATP8A2-R	TTGTTGAGATGCGGTTGGTTGAG
hsa-NPY-F	GCGACACTACATCAACCTCATCAC
hsa-NPY-R	AGGGTCTTCAAGCCGAGTTCTG
hsa-C1orf198-F	GTTCTTGTTGCTTATGTGACCTGTTG
hsa-C1orf198-R	ATGCTGGAAGACTCTAACACAACTAAG
hsa-MYOC-F	CAGTCAGTCGCCAATGCCTTC
hsa-MYOC-R	GATACCTGTGCCTGTGTCATAAGC
hsa-ADH1A-F	GGCTCTACCTGTGCTGTGTTTG
hsa-ADH1A-R	TGATGTCCACCGCAATGATTCTG
hsa-SYT16-F	ATATAGAGCCGCCAGCCAGAAG
hsa-SYT16-R	TCTTACCAGGCAGCAGCACTAC
hsa-CCL5-F	ATATGGCTCGGACACCACTC
hsa-CCL5-R	TCCTTCGAGTGACAAACACG
hsa-CSF2-F	GCATGTAGAGGCCATCAAAGA
hsa-CSF2-R	CGGGTCTGCACACATGTTA
hsa-CD86-F	CACTATGGGACTGAGTAACATTC
hsa-CD86-R	GCACTGACAGTTCAGAATTCATC
hsa-β-actin-F	CAGATGTGGATCAGCAAGCAGGAG
hsa-β-actin-R	CGCAACTAAGTCATAGTCCGCCTAG

Elisa

We used Human IL-6 ELISA Kit (Beyotime, PI325), Human IFN-γ ELISA Kit (Beyotime, PI511) and Human cGMP ELISA Kit (jonln, JL11898-96T) for corresponding protein expression detection.

Cck-8

Cells were inoculated into 12-well plates, with 6000 cells per well, and cultured for 48 h. Subsequently, 10 μL of CCK8 reagent (Beyotime, C0037) was added for incubation in an incubator at 37°C for 2 h, following which the detection area was selected and the OD value was detected by setting the wavelength of the enzyme labeler at 450 nm for the evaluation of cell activity.

EdU

Cells were inoculated into 12-well plates, with 6000 cells per well, and cultured overnight to restore them to normal state. Subsequently, 2×EdU working solution (Beyotime, C0071S) was added for incubation in an incubator at 37°C for 2 h. Next, 1 mL of fixing solution was added for another 15 min of incubation, followed by continuous 30-min incubation after the addition of Click reaction solution. Finally, the cells were observed and recorded under a fluorescence microscope to evaluate their proliferation.

Tunel

Apoptosis was evaluated using the TUNEL apoptosis assay kit (Beyotime, C1091). After being fixed with 4% paraformaldehyde for 30 min, the cells were incubated with PBS containing 0.3% Triton X-100 at room temperature for 5 min. Subsequently, they were incubated with 0.3% H_2O_2 in PBS at room temperature for 20 min. Next, 50 μL of prepared biotin labeling solution was added for a 60-min follow-up incubation at 37°C under light-protected conditions. Finally, DAB color solution was used to color development.

Scratch Wound Healing Assay

On the single-layer adherent cells cultured in dishes, we marked the central region of cell growth with a micro gun head to remove the central part of the cells. Subsequently, cells were cultured in serum-free medium, and cell migration was assessed by observing the extent to which surrounding cells migrated to the central scratch area under a microscope.

Transwell Assay

We coated the upper chamber surface of the bottom membrane of the transwell chamber with matrigel matrix glue, and after solidification, 100 μL of cell suspension was added to the upper chamber, and culture medium to the lower chamber. After 24 h of routine cell culture in the cell incubator, the cells were stained with crystal violet, and cell invasion was determined by observing the cell count in the field of vision under a microscope.

Detection of Macrophages

We labeled cells with purified anti-human CD86 Antibody (Biolegend, 374202) and used flow cytometry to observe M1 macrophages and calculate the cell proportion of M1 macrophages.

Statistical Analysis

Statistical analysis of the bioinformatics analysis, along with result visualization, was conducted using R, with between-group comparisons performed using Wilcox. The experimental analysis and corresponding data presentation were carried out using GraphPad Prism 9, with between-group comparisons assessed using *t*-tests. All data are presented as mean ($\bar{x}$) ± standard deviation (SD). All experiments were performed with three biological replicates.

Results

Figure 1 illustrates the study's methodology.

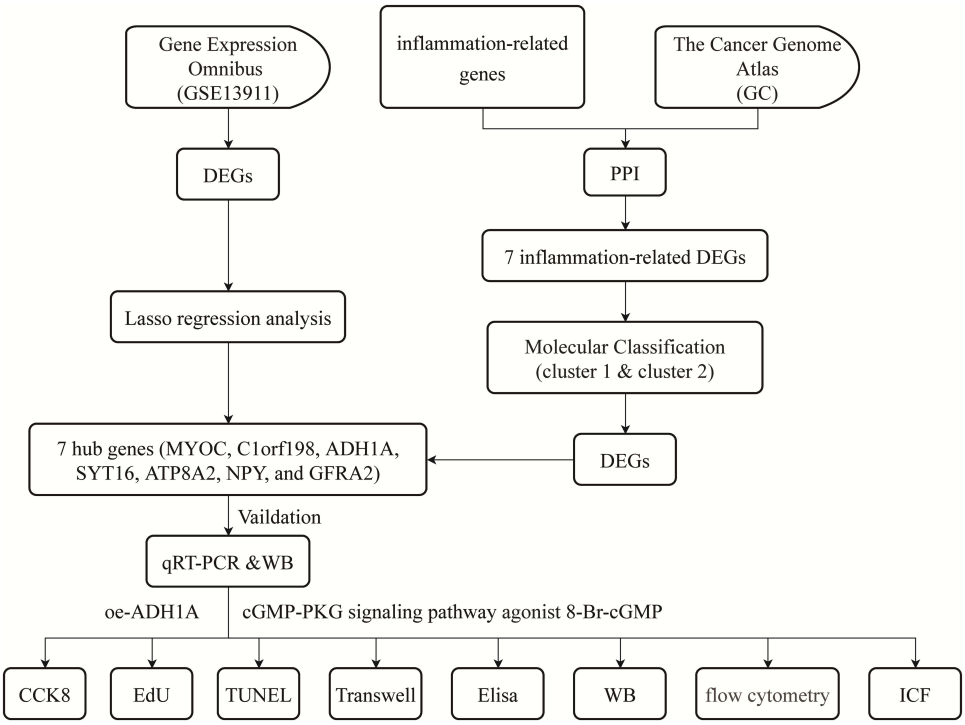

Figure 1 Study flowchart.

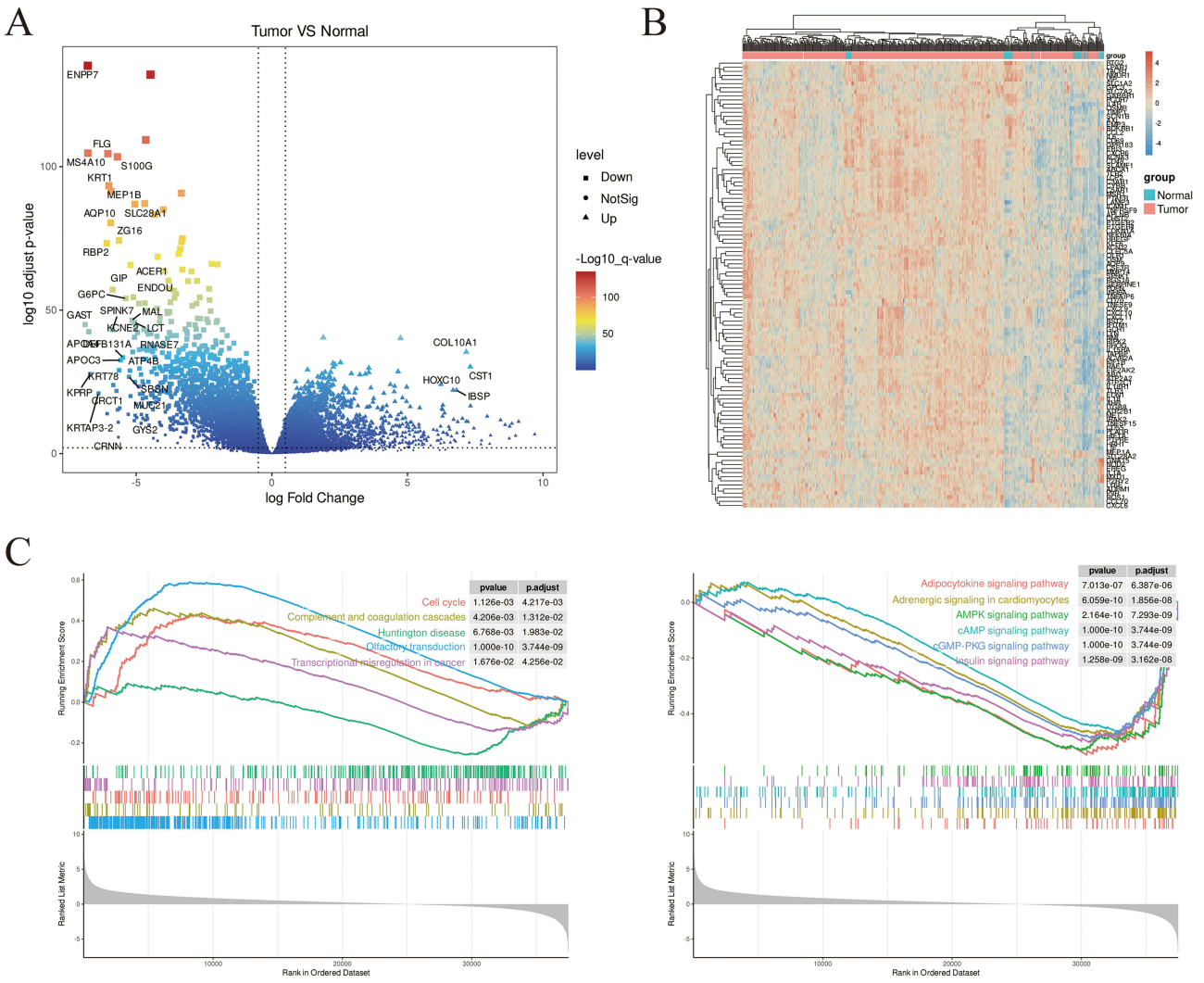

Figure 2 Differential analysis. (**A**) The volcano plot shows the results of the differential analysis; (**B**) The heatmap shows the expression of the top 40 genes in the down-regulated and up-regulated DEGs, respectively; (**C**) Functional enrichment analysis of all genes.

Differential Analysis

By conducting differential analysis of the GC datasets downloaded from the TCGA database, we screened out 11975 differentially expressed genes (DEGs) according to the criterion of $|\log_2 FC|>1$ and adjust. p-value <0.05, comprising 5389 up-regulated and 6586 down-regulated DEGs. The results were presented with a volcano plot (Figure 2A), and the top 40 genes from both up- and down-regulated DEGs were selected for heatmap plotting (Figure 2B). Thereafter, functional enrichment analysis of the genes revealed activation of cell cycle, complement and coagulation cascades, and transcriptional misregulation in cancer in the disease group, while the adipocytokine pathway, AMPK signaling and insulin pathway were inhibited (Figure 2C).

Screening for Inflammation-Related DEGs

We downloaded 200 inflammation-related genes involved in the HALLMARK_INFLAMMATORY_RESPONS and intercrossed them with DEGs from the TCGA dataset, obtaining 109 inflammation-related DEGs (Figure 3A). To further screen key genes, PPI analysis was conducted on these inflammation-related DEGs, and MCC, MNC, DMNC, Degree, and EPC methods were respectively applied (Figure 3B). We selected the top 20 key genes for intersection (Figure 3C), and identified 7 inflammation-related DEGs: IL-18, TIMP1, CCL20, CXCL11, CXCL9, TLR3 and NOD2. Among them, IL-18, TIMP1,

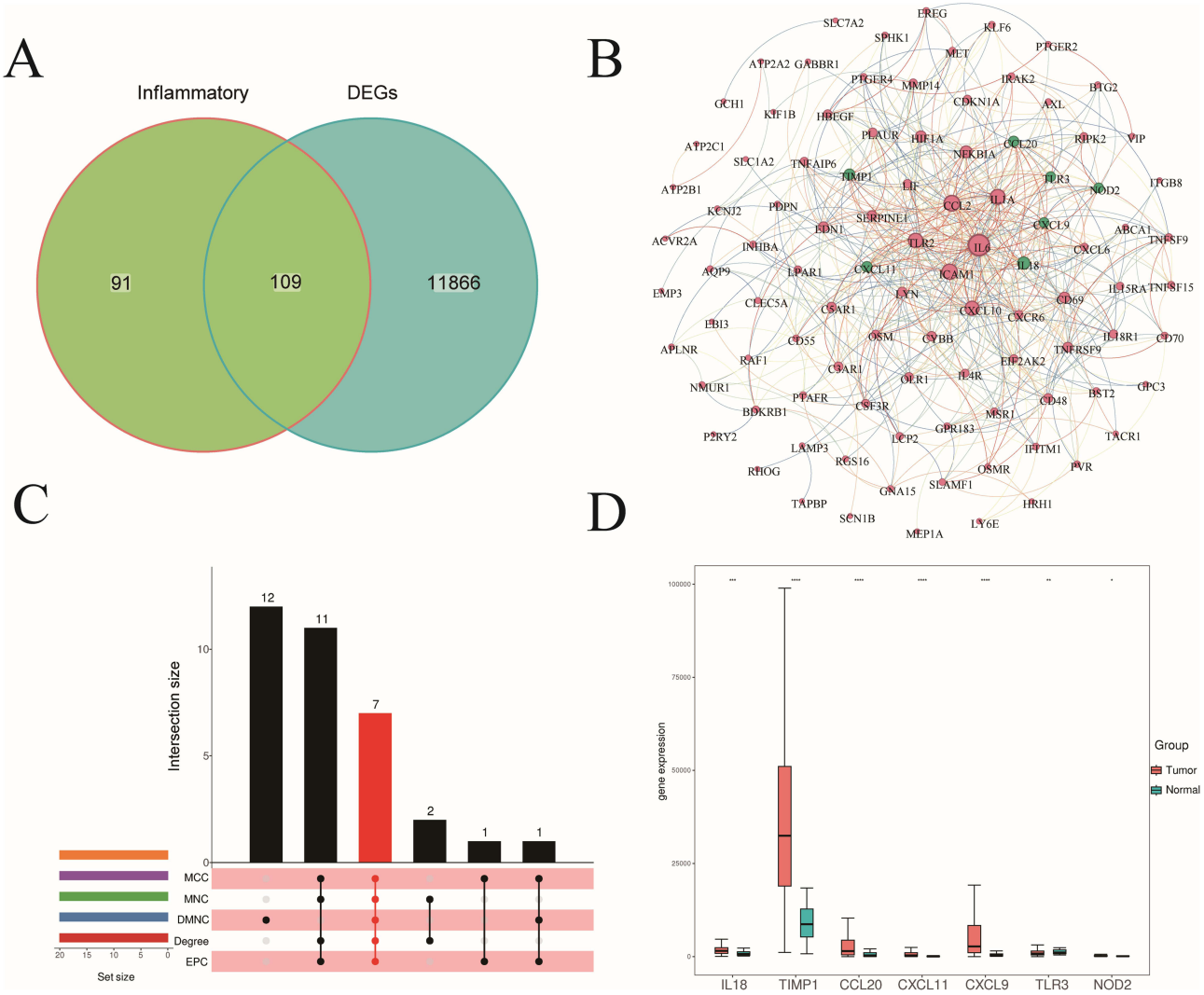

Figure 3 Screening for inflammation-related DEGs. (**A**) Venn diagram; (**B**) PPI network diagram (The seven selected inflammation-related DEGs are marked in green, and the other genes are marked in pink); (**C**) Upset diagram; (**D**) Expression box plot of key inflammation-related DEGs.

CCL20, CXCL11 and CXCL9 were highly expressed in the disease group, while TLR3 and NOD2 were lowly expressed (Figure 3D).

Molecular Typing of GC

Based on the expression of 7 inflammation-related DEGs, the disease samples in the TCGA dataset were typed and clustered into two subtypes, namely Cluster 1 and Cluster 2, comprising 233 and 177 samples, respectively (Figure 4A). Through subsequent differential analysis of Cluster 1 and Cluster 2, 8174 DEGs were identified with $|\log_2 FC|>1$ and adjust. p-value <0.05, of which 4116 were up-regulated and 4058 were down-regulated (Figure 4B and C). Functional analysis revealed the potential involvement of these DEGs in the p53 signaling pathway, estrogen signaling pathway, and inflammatory mediator regulation of TRP channels, etc (Figure 4D).

Immune Infiltration Analysis

Immune infiltration analysis was performed on the TCGA dataset, and samples with significant immune infiltration results ($p<0.05$) were retained. A total of 216 disease and 29 control samples were included in subsequent analysis (Figure 5A). Notably, significant differences in T cells CD4 memory resting, NK cells resting, Macrophages M1, T cells regulatory Tregs, plasma cells, T cells follicular helper, B cells memory, T cells CD4 memory activated, and naïve B cells were observed

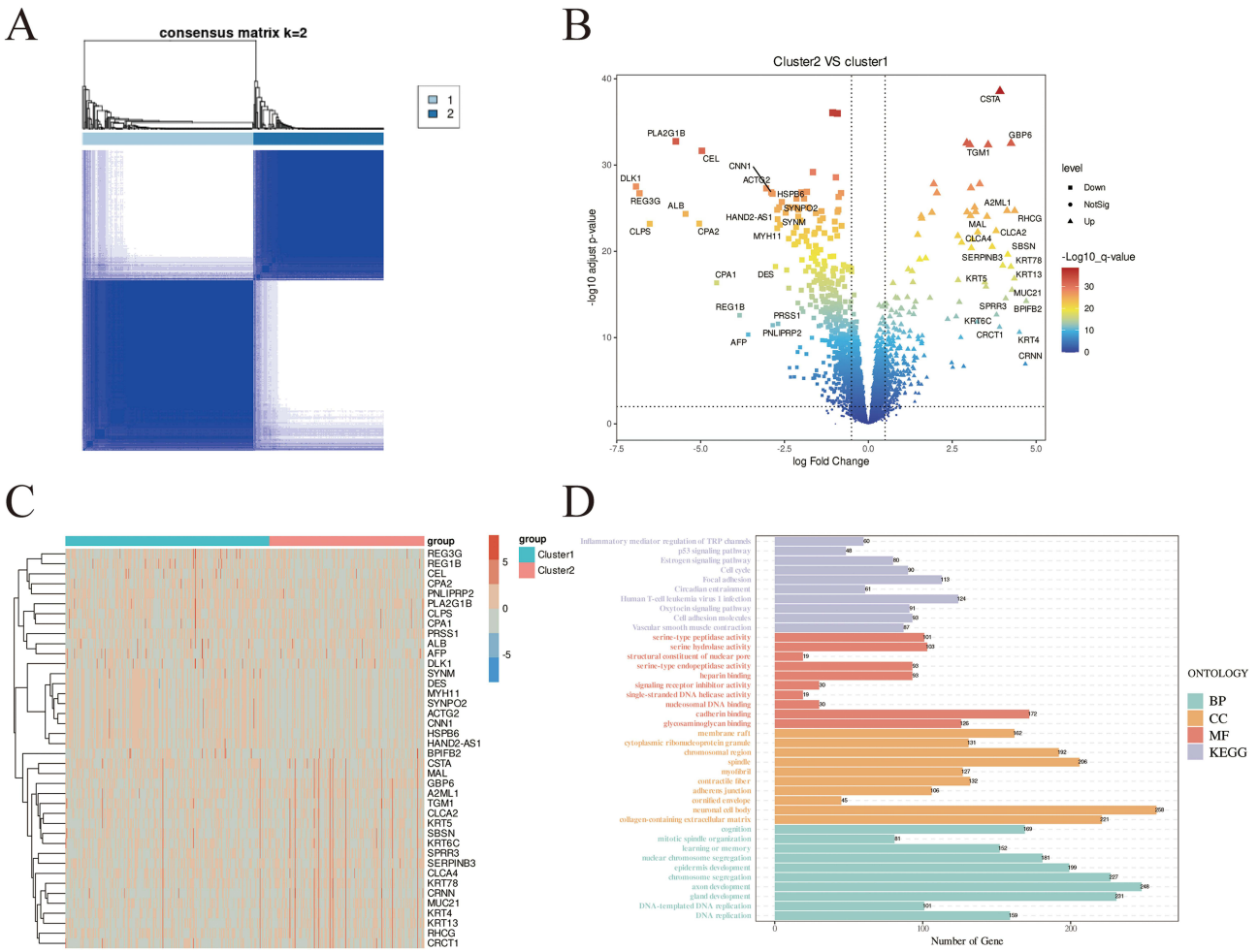

Figure 4 Molecular typing of GC. (**A**) Clustering heatmap at K=2; (**B**) The volcano plot shows the results of the differential analysis; (**C**) Clustering heatmap showing the expression of DEGs; (**D**) Functional enrichment analysis of DEGs.

between Cluster 1 and Cluster 2 (Figure 5B). Correlation analysis revealed significant correlations between the 7 inflammation-related DEGs and immune cells in both Cluster 1 and Cluster 2 (Figure 5C and D). Thus, we hypothesized that these 7 inflammation-related DEGs may be closely related to immune responses in the tumor microenvironment.

Screening of Hub Genes

By conducting differential analysis on the GSE13911 dataset, a total of 7476 DEGs were screened out based on the criteria of $|\log_2 FC|>1$ and p-value <0.05, comprising 4195 up-regulated and 3281 down-regulated DEGs (Figure 6A and B). Functional analysis revealed their main enrichment in ribonucleoprotein complex biogenesis, DNA replication and mitotic nuclear division (Figure 6C), as well as pathways including the P53 signaling pathway, nucleotide excision repair, and mRNA surveillance pathway (Figure 6D). Thereafter, by performing Lasso regression analysis, 28 key genes were identified from the DEGs in the GSE13911 dataset (Figure 6E and F). After taking intersection of these key genes with the DEGs between Cluster 1 and Cluster 2 (Figure 6G), 10 intersected genes (NUTF2, MYOC, NAA15, C1orf198, ADH1A, SYT16, ATP8A2, NPY, GFRA2 and EDC4) were obtained. Wilcox test was used to determine whether these 10 intersected genes were significantly different in the TCGA (Figure 7A) and GSE13911 datasets (Figure 7B), respectively, and MYOC, C1orf198, ADH1A, SYT16, ATP8A2, NPY, and GFRA2 were found to be significantly different in both datasets. These 7 hub genes were further analyzed through bioinformatics analysis. ROC analysis demonstrated their role in distinguishing tumor samples from control samples in the GSE13911 dataset (Figure 7C).

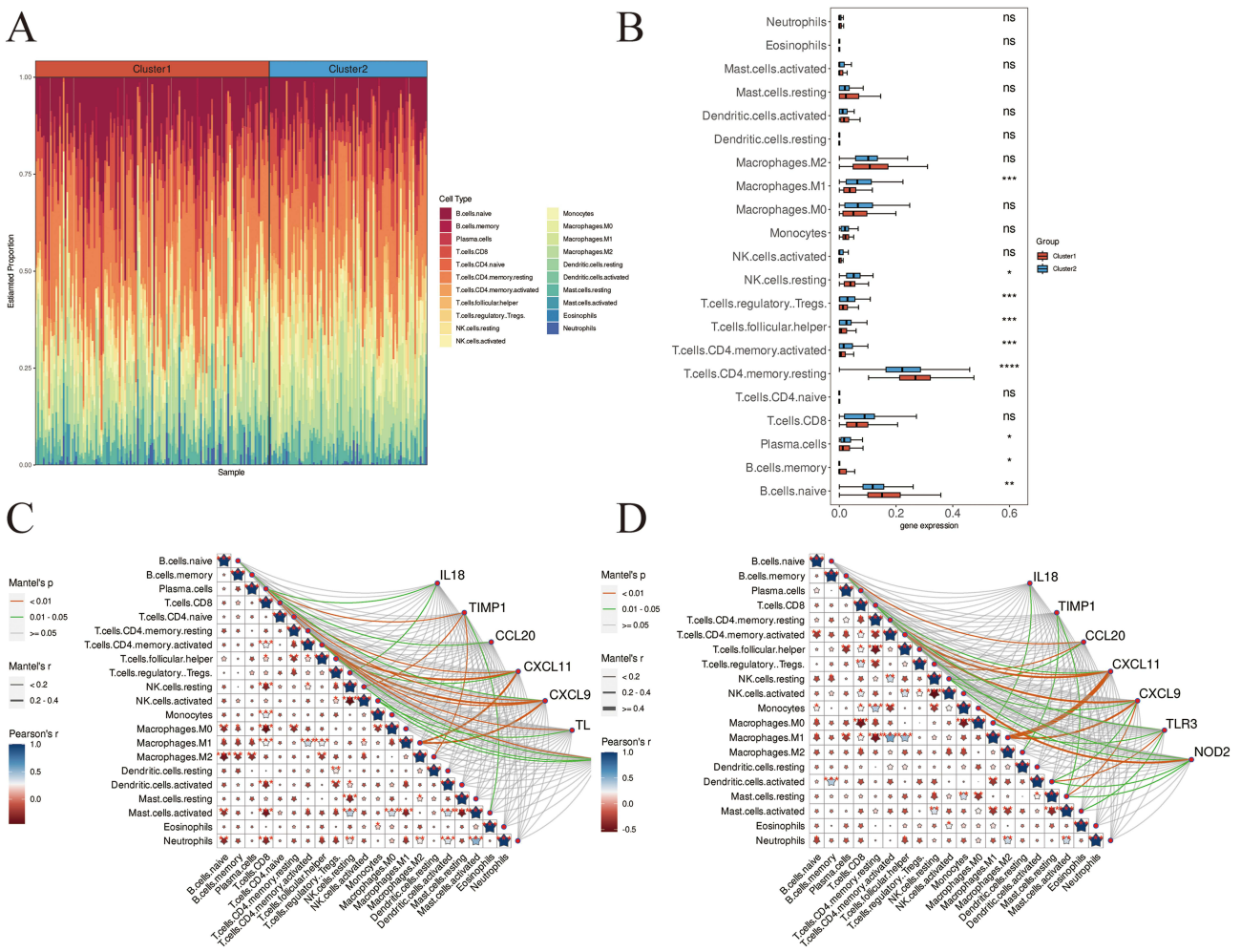

Figure 5 Immune infiltration analysis. (**A**) Proportion of immune cells in each sample; (**B**) Differential analysis of immune cells in Cluster 1 and Cluster 2 groups; (**C**) Correlation between key inflammation-related DEGs and immune cells, as well as correlation between immune cells in Cluster 1. (**D**) Correlation between key inflammation-related DEGs and immune cells, as well as correlation between immune cells in Cluster 2.

Analysis of Hub Gene Expression in GC Cells

The validation of hub gene expression in GC cell lines through qRT-PCR revealed decreased expression of MYOC, ADH1A, and NPY, and increased expression of GFRA2 in GC cells compared with GES-1 (Figure 8A). Notably, the expression trend of ADH1A was consistent with the results obtained by bioinformatics analysis, and WB experiment further confirmed a significant reduction of ADH1A in GC cells (Figure 8B). Given the lack of previous studies on ADH1A, we chose ADH1A for carrying out subsequent functional study.

Impact of ADH1A on GC Cells

To elucidate the mechanism of action of ADH1A, we overexpressed ADH1A in AGS and HGC-27 cells (Figure 9A). In comparison with the AGS+oe-NC group, the AGS+oe-ADH1A group demonstrated significantly decreased cell activity (Figure 9B) and cell proliferation (Figure 9C), along with markedly reduced migration (Figure 9D) and invasion (Figure 9E), coupled with a notable increase in apoptosis (Figure 9F). Similarly, in HGC-27 cells, overexpression of ADH1A resulted in inhibition of cell activity, proliferation, migration and invasion, while promoting apoptosis. Concurrently, we detected a significant increase in the secretion of IL-6, IFN-γ, CCL5 and CSF2 by GC cells following overexpression of ADH1A (Figure 9G and H).

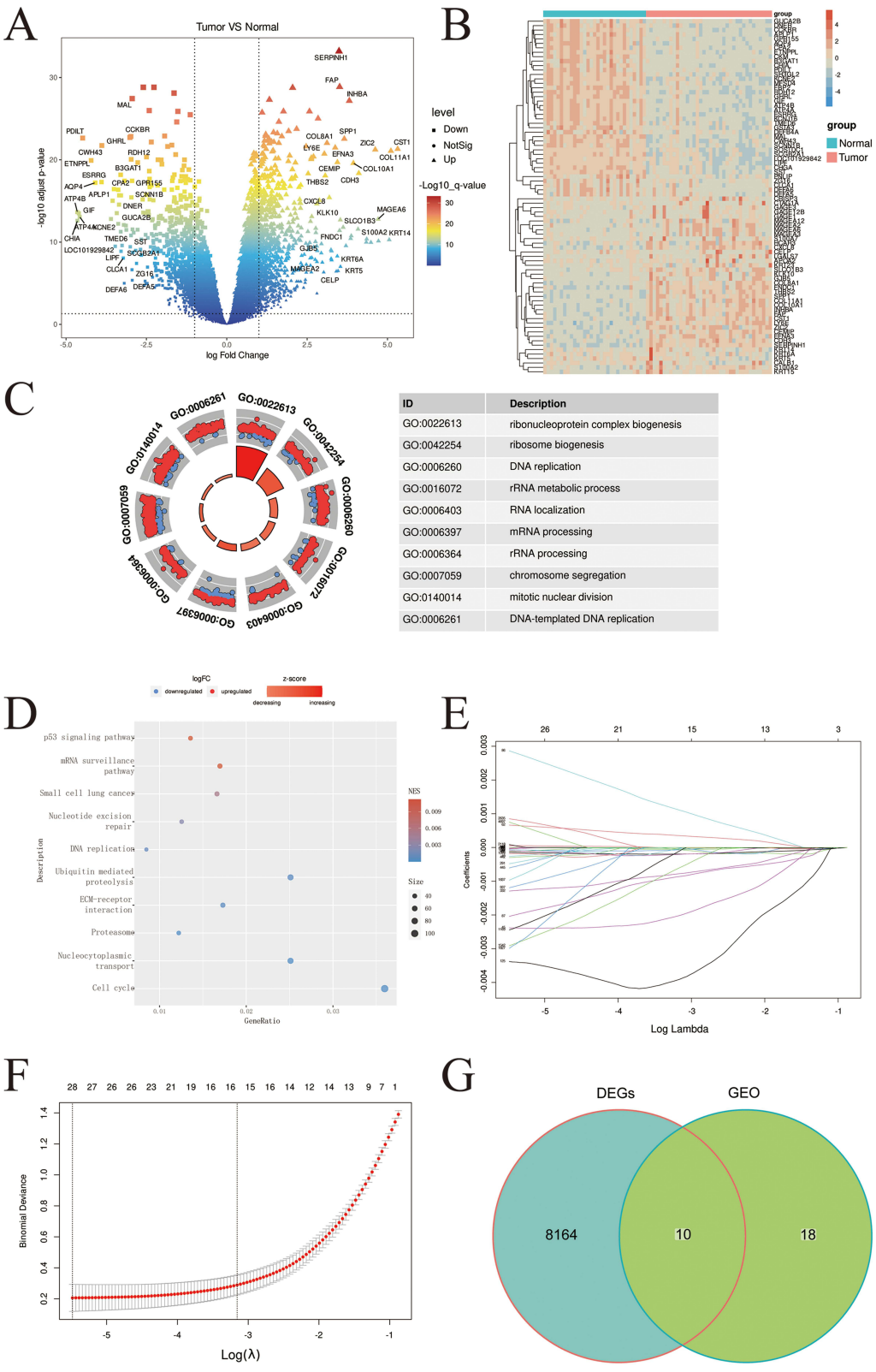

ID	Description
GO:0022613	ribonucleoprotein complex biogenesis
GO:0042254	ribosome biogenesis
GO:0006260	DNA replication
GO:0016072	rRNA metabolic process
GO:0006403	RNA localization
GO:0006397	mRNA processing
GO:0006364	rRNA processing
GO:0007059	chromosome segregation
GO:0140014	mitotic nuclear division
GO:0006261	DNA-templated DNA replication

Figure 6 Differential analysis. (**A**) Volcano map; (**B**) Heatmap; (**C**) GO analysis; (**D**) KEGG analysis; (**E**) Calculation of regression coefficients; (**F**) Best Predictive Model; (**G**) Venn diagram.

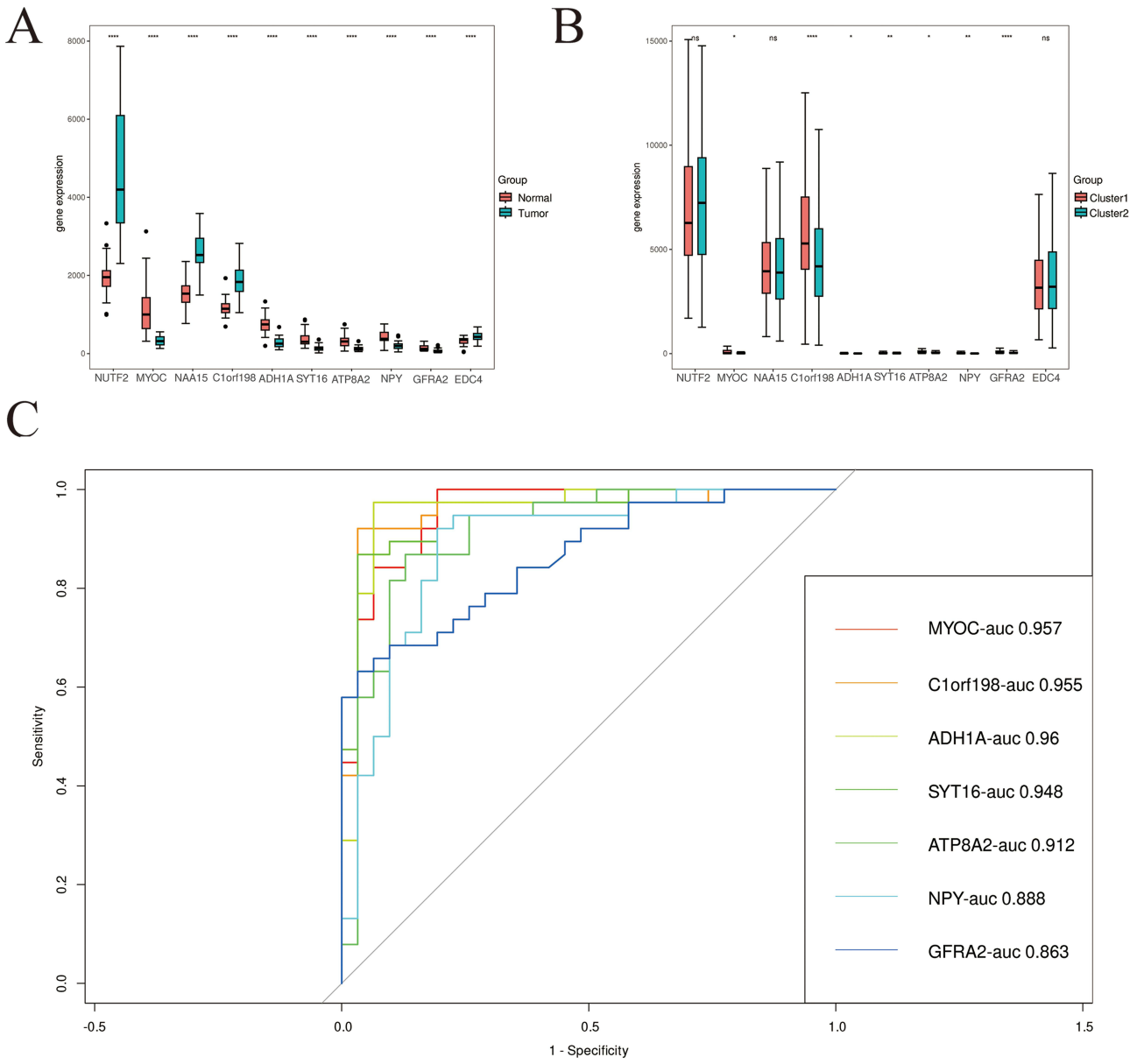

Figure 7 Hub gene. (**A**) Expression box plots of intersecting genes in Cluster 1 and Cluster 2; (**B**) Expression box plots of intersecting genes in the GSE13911 dataset; (**C**) ROC analysis based on each of the seven hub genes in the GSE13911.

ADH1A Enhances the Polarization of M1 Macrophage Phenotype

After overexpressing ADH1A, we found an increase in the secretion of IFN-γ by GC cells, so we speculated that the cells in AGS+oe-ADH1A and HGC+oe-ADH1A groups may promote the polarization of macrophages to M1 type. To verify our hypothesis, we cultured macrophage THP-1 with the culture supernatants collected from the AGS+oe-ADH1A, AGS +oe-NC, HGC-27+oe-ADH1A, and HGC-27+oe-NC groups, and found that high expression of ADH1A in GC cells promoted THP-1 migration (Figure 10A). Meanwhile, both flow cytometry (Figure 10B) and qRT-PCR results (Figure 10C) demonstrated that high expression of ADH1A in GC cells could significantly increase the proportion of M1 macrophages. Thus, ADH1A can enhance the polarization of M1 macrophage phenotype.

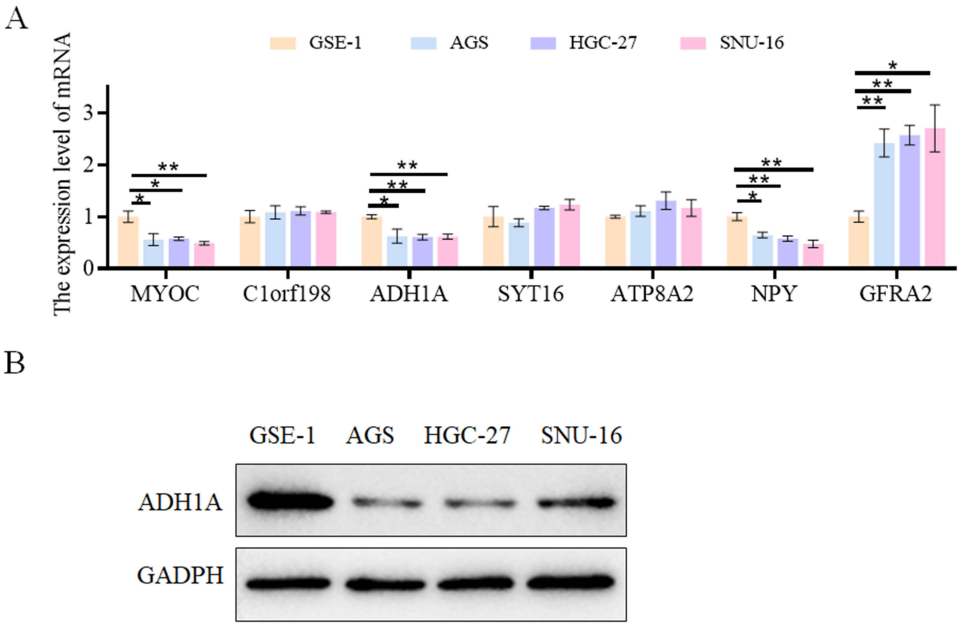

Figure 8 Expression analysis of hub gene in GC cell lines. (**A**) The expression levels of MYOC, ADH1A, NPY and GFRA2; (**B**) The expression level of ADH1A protein.
Notes: *p<0.05, **p<0.01.

ADH1A Affects the Malignant Progression of GC Through the cGMP-PKG Signaling Pathway

ssGSEA on ADH1A revealed the potential involvement of ADH1A in the cGMP-PKG signaling pathway (Figure 11A). Therefore, we examined the expression of proteins related to the cGMP-PKG signaling pathway in GSE-1, AGS and HGC-27 cells, revealing a significant increase in the protein levels of PKG1, PKG2, pVASP, and cGMP in AGS and HGC-27 cells (Figure 11B and C). However, upon overexpressing ADH1A in AGS and HGC-27 cells, the protein levels of PKG1, PKG2, pVASP and cGMP in the cells were significantly decreased (Figure 11B and C). To clarify the role of the cGMP-PKG signaling pathway in GC progression, we treated HGC-27+oe-ADH1A cells with the cGMP-PKG signaling pathway agonist 8-Br-cGMP (Figure 11B). Compared with the HGC-27+oe-ADH1A group, the HGC-27+oe-ADH1A+8-Br-cGMP group showed significantly increased levels of cell activity (Figure 11D), proliferation (Figure 11E), migration and invasion (Figure 11F and G), but notably decreased apoptosis level (Figure 11H). Moreover, the expression levels of IL-6, IFN-γ, CCL5 and CSF2 were significantly decreased in the HGC-27+oe-ADH1A+8-Br-cGMP group (Figure 11I and J). At the same time, the supernatant of GC cells was collected and co-cultured with THP-1. It was found that the migration of THP-1 in the HGC-27+oe-ADH1A+8-Br-cGMP group was significantly decreased (Figure 12A), and the proportion of M1 macrophages was significantly decreased (Figure 12B and C). Therefore, we concluded that ADH1A can influence the malignant progression of GC and the transformation of macrophages into the pro-inflammatory M1 phenotype by regulating the cGMP-PKG signaling pathway.

Discussion

Inflammation and immune cell dysfunction in the tumor microenvironment are critical factors influencing GC development.[9] Inflammation is a double-edged sword, for anti-inflammatory drugs (aspirin, statins, etc.)[10] can significantly reduce cancer morbidity and mortality, whereas pro-inflammatory factors (TNF-α, cGAS-STING pathway activators, etc.) can improve tumor outcome by promoting immune cell infiltration into infected tissues.[11] Acute inflammation in the tumor microenvironment induces an anti-tumor immune response leading to cancer cell death,[12] whereas chronic inflammation suppresses the immune response, creating a tumor inflammatory microenvironment conducive to tumorigenesis, progression and metastasis. Recognizing the tumor inflammatory microenvironment as

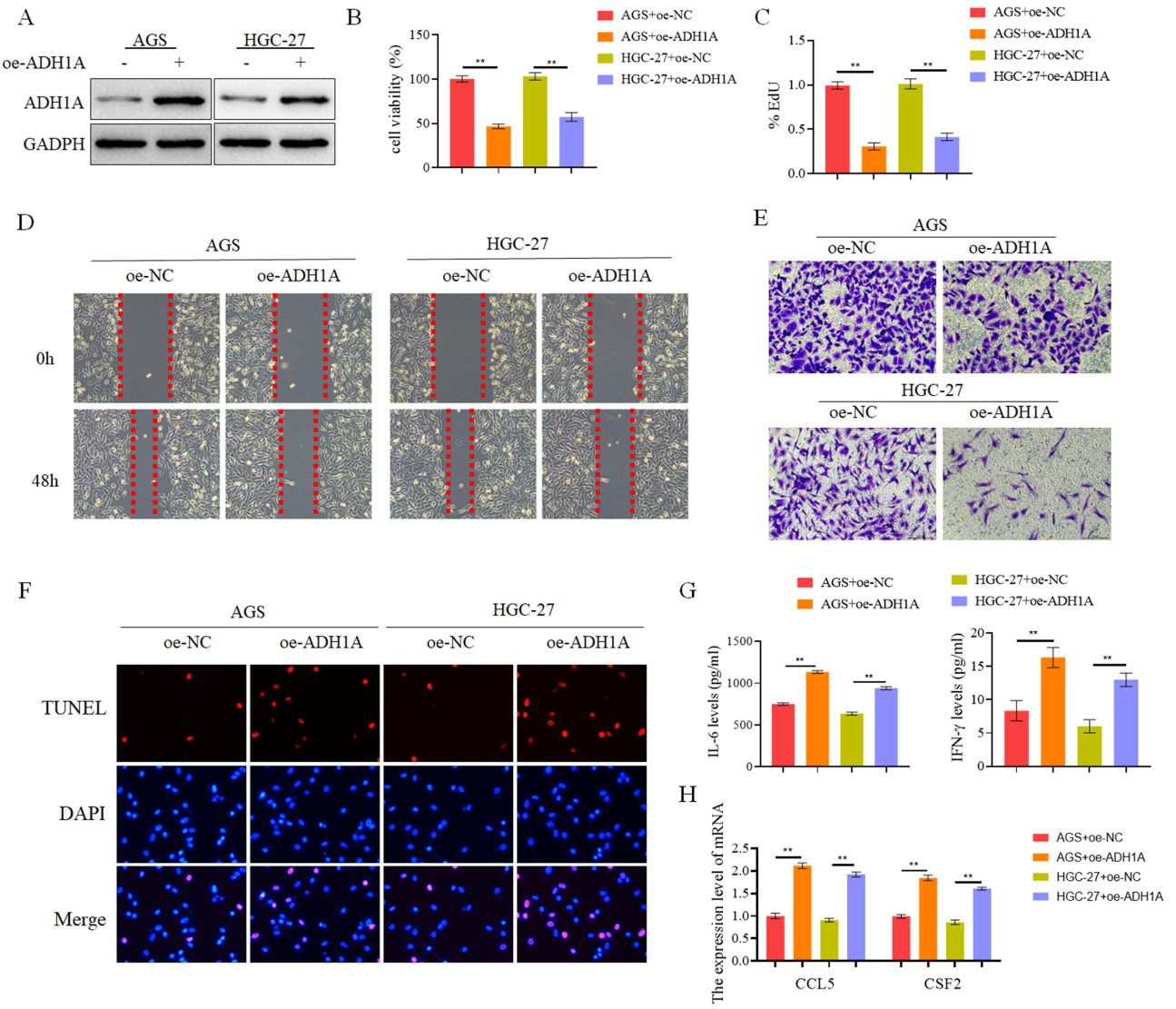

Figure 9 Effect of ADH1A on GC cells. (**A**) The expression of ADH1A in the cells; (**B**) Detection of cell activity; (**C**) Detection of cell proliferation; (**D**) Cell migration ability; (**E**) Cell invasion ability; (**F**) Apoptosis level; (**G**) The expression of IL-6 and IFN-γ; (**H**) The expression of CCL5 and CSF2.
Notes: **$p<0.01$.

a key determinant of improved immunotherapy efficacy,[13] the current study expects to identify new inflammation-related targets to modulate immune responses, ultimately improving the efficacy of cancer immunotherapy.

This study screened out 7 inflammation-related DEGs that may affect the development of GC, namely IL-18, TIMP1, CCL20, CXCL11, CXCL9, TLR3, and NOD2, by bioinformatics. Pro-inflammatory cytokines IL-18[14] and TLR3[15] are prognostic indicators for GC, while TIMP1[16] and NOD2[17] are involved in the malignant progression of GC. Additionally, C-X-C motif ligand (CXCL) play important roles in the tumor microenvironment, where chemokine CCL20 regulates the tumor microenvironment in a variety of malignant tumors, including hepatocellular carcinoma, colon cancer, breast cancer, pancreatic cancer and GC.[18,19] The CXCL family predicts GC development[20] and regulates immune responses in the tumor microenvironment, with CXCL11 influencing T cell recruitment in the bloodstream and in tumors by modulating PD-L1-induced immunosuppressive signaling,[21] and CXCL9 promoting the development of immune escape.[22] These DEGs, indicating predictive or regulatory roles in GC progression, led us to molecularly type the disease samples based on the 7 inflammation-related DEGs into two groups, Cluster 1 and Cluster 2, for subsequent studies.

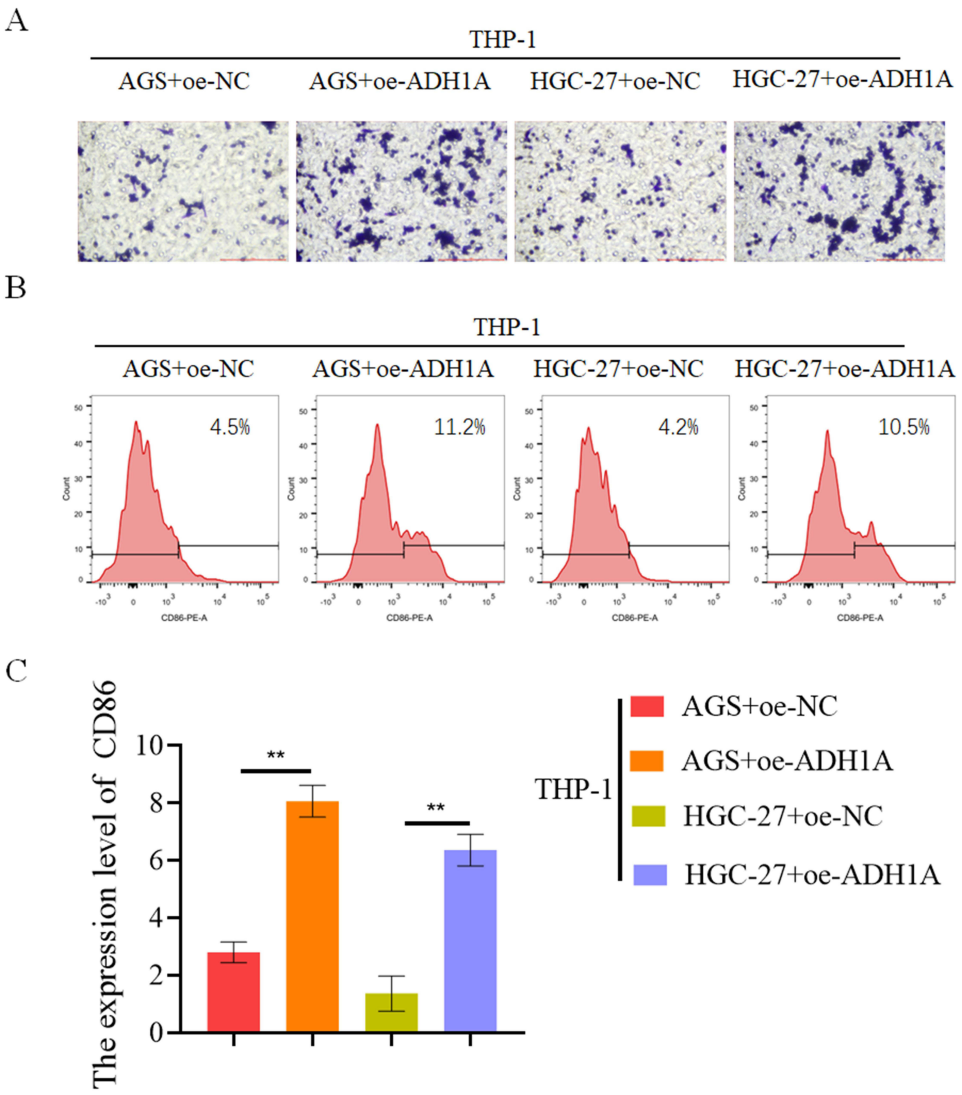

Figure 10 ADH1A enhances the polarization of macrophage M1 phenotype. (**A**) Cell migration ability was detected; (**B**) The proportion of M1 was detected by flow cytometry; (**C**) M1 macrophage marker CD86 was detected.
Notes: **$p<0.01$.

Immune infiltration analysis of samples from both Cluster 1 and Cluster 2 revealed the potential key role of immune cells, including Macrophages M1, T cells regulatory Tregs, NK cells resting, T cells follicular helper, plasma cells, T cells CD4 memory resting, B cells memory, T cells CD4 memory activated, and B cells naïve, in GC progression. Notably, while TAMs secrete CXCL1 and CXCL5 to promote GC cell migration, GC cells also secrete TNF-α to further induce TAMs to secrete CXCL1 and CXCL5;[23] TAMs can also induce mesenchymal stem cells to acquire cancer-related fibroblast-like features and pro-inflammatory phenotypes, remodel the inflammatory microenvironment, and enhance the oncogenic transformation of gastric epithelial cells;[24] and TAM also influence resistance to tumor immunotherapy.[25,26] Therefore, TAM has also become a hot topic in the study of tumor microenvironment. Lymphocytes can be divided into NK cells, T cells and B cells according to their functions, among which NK cells can directly target and lyse malignant cells, and can also coordinate the anti-tumor immune response by recruiting adaptive and innate leukocytes, but it is unclear whether they can regulate the tumor microenvironment and improve the efficacy of immunotherapy.[27] Regulatory T cells differentiated from T cells are able to suppress inflammation,[28] aiding cancer cells in escaping the immune system.[29] Likewise, regulatory B cells differentiated by B cells can also regulate the immune microenvironment and influence the inflammatory response in the immune system.[30] The above results not only prove the scientific and rational

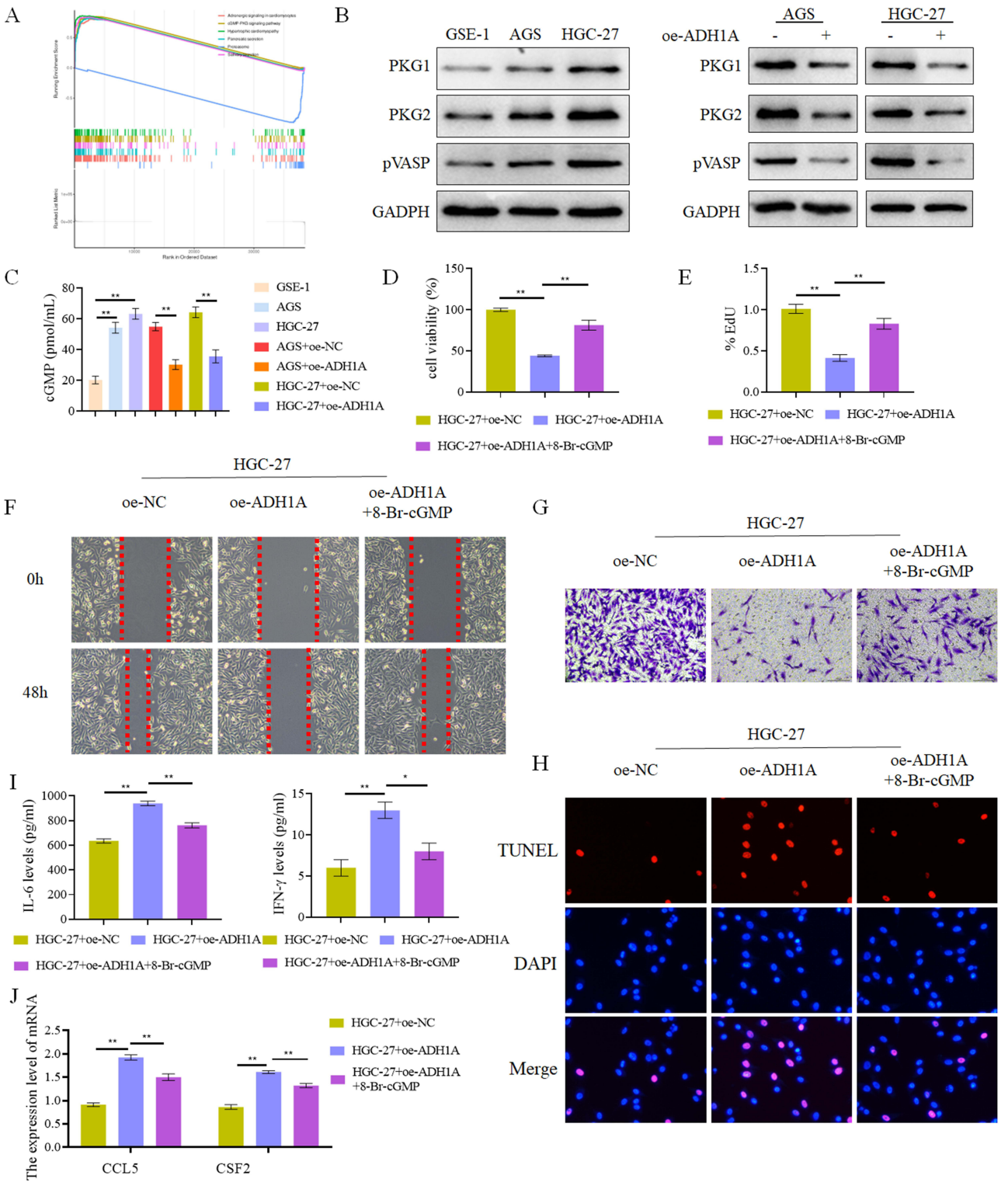

Figure 11 ADH1A affects the malignant progression of GC through the cGMP-PKG signaling pathway. (**A**) Results of ssGSEA of ADH1A; (**B**) The expression levels of PKG1, PKG2, pVASP and VASP protein; (**C**) The expression of cGMP; (**D**) Detection of cell activity; (**E**) Detection of cell proliferation; (**F**) Cell migration ability; (**G**) Cell invasion ability; (**H**) Apoptosis level; (**I**) The expression of IL-6 and IFN-γ; (**J**) The expression of CCL5 and CSF2.
Notes: *p<0.05, **p<0.01.

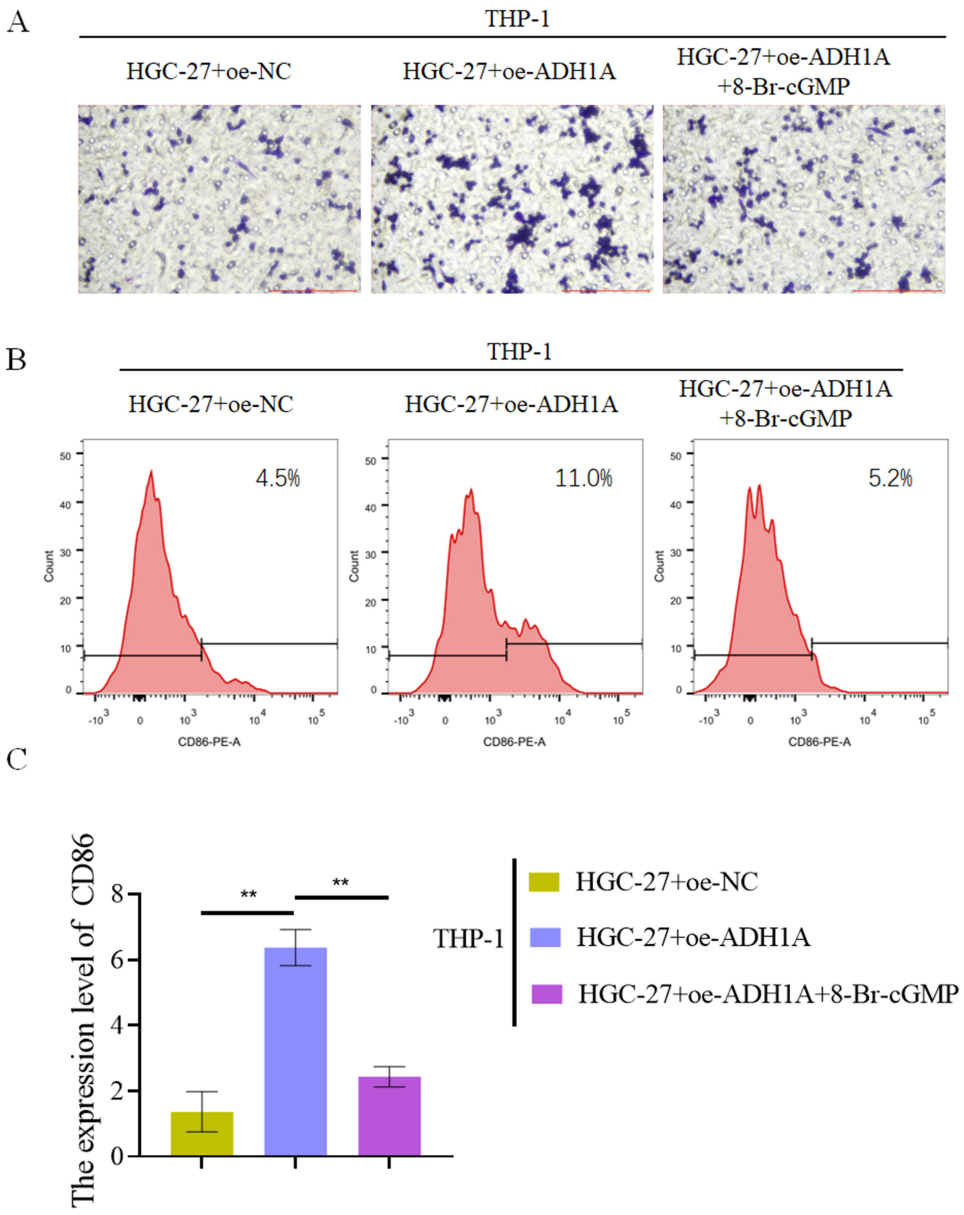

Figure 12 ADH1A affects the transformation of macrophages to pro-inflammatory M1 phenotype through the cGMP-PKG signaling pathway. (**A**) Cell migration ability was detected; (**B**) The proportion of M1 was detected by flow cytometry; (**C**) M1 macrophage marker CD86 was detected.
Notes: $^{**}p<0.01$.

grouping of Cluster 1 and Cluster 2, but also suggest the crucial role of inflammation-induced immune cell changes in the progression of GC within the tumor microenvironment.

Thereafter, our study screened out 7 hub genes, MYOC, C1orf198, ADH1A, SYT16, ATP8A2, NPY, and GFRA2, from the GSE13911 dataset, which are associated with inflammation and affect GC progression. NPY and MYOC are recognized regulators of inflammation,[31,32] with NPY exerting pro-inflammatory effects by recruiting immature dendritic cells during the immune/inflammatory response, while also displaying anti-inflammatory effects by promoting T helper 2 polarization.[33] As reported, low expression of NPY in the plasma of GC patients may reflect the progression of GC,[34] but there have been currently no studies on inflammation or mechanisms of action in GC. MYOC has been found in glaucoma disease where MYOC mutants can activate the inflammatory response, while wild-type MYOC has anti-inflammatory activity.[32] In addition, MYOC is also involved in muscle atrophy and dysfunction induced by pancreatic ductal adenocarcinoma, resulting in the occurrence of cancer cachexia and seriously affecting the prognosis of cancer

patients.[35] Although MYOC has not been studied in GC, related cancers of the pancreas, esophagus, stomach, lung, liver, and intestine are highly associated with the occurrence of cancer cachexia. We hypothesize that MYOC may affect the prognosis of GC. Although ADH1A and GFRA2 have not been studied in GC, ADH1A has been found to inhibit the progression of non-small cell lung cancer[36] and hepatocellular carcinoma,[37] while GFRA2 has been found to promote the development of neuroblastoma[38] and pancreatic cancer.[39]

To verify whether these 7 genes can predict GC progression, qRT-PCR was carried out and revealed decreased MYOC, ADH1A and NPY expression as well as significantly increased GFRA2 expression in GC cells. Given that the expression trend of ADH1A is consistent with corresponding bioinformatics results, we chose ADH1A for subsequent biological research. To verify the function of ADH1A, we overexpressed ADH1A in GC cells and found that overexpression of ADH1A inhibited the activity, proliferation, migration and invasion of GC cells, promoted apoptosis and the secretion of IL-6, IFN-γ, CCL5 and CSF2, and inhibited the transformation of macrophages into pro-inflammatory M1 phenotype. Bioinformatics analysis indicated ADH1A's involvement in the cGMP-PKG signaling pathway, and overexpression of ADH1A in GC cells affected the changes of proteins related to the cGMP-PKG signaling pathway. Therefore, we used the cGMP-PKG signaling pathway activator for further verification, and confirmed that ADH1A can affect the malignant progression of GC and the transformation of macrophages to pro-inflammatory M1 phenotype by regulating the cGMP-PKG signaling pathway.

There are still limitations in the current study. First and foremost, we only investigated the mechanism of ADH1A's impact on the function of GC cells at the cellular level, and further validation at the animal level is necessary to clarify the mechanism of action of ADH1A in GC. Additionally, more clinical samples are required to further elucidate the clinical diagnostic or therapeutic role of ADH1A.

Conclusion

This study integrated GC-related datasets from TCGA and GEO databases using bioinformatics methods, identifying inflammation-related genes (ADH1A, NPY, MYOC and GFRA2) that affect GC progression. At the cellular level, ADH1A was found to regulate the transformation of macrophages to pro-inflammatory M1 phenotype and malignant progression of GC through the cGMP-PKG signaling pathway. Our findings provide a novel immunotherapeutic target for GC, and establish a corresponding scientifically rigorous theoretical basis.

Abbreviations

GC, Gastric cancer; ICIs, Immune checkpoint inhibitors; ICs, Immune checkpoints; TAMs, Tumor-associated macrophages; MSigDB, Molecular Signatures Database; GSEA, gene set enrichment analysis; PPI, Protein-protein interaction; ROC, receiver operating characteristic curve; FBS, fetal bovine serum; SD, Standard deviation; DEGs, Differentially expressed genes.

Data Sharing Statement

Data are available from the corresponding author on reasonable request.

Ethics Approval and Consent to Participate

The Cancer Genome Atlas (TCGA), Gene Expression Omnibus (GEO), and Molecular Signatures Database (MSigDB) are public databases that allow unlimited reuse under open licenses. Ethics approval had been obtained prior to the conduction of the study involving patients included in these databases. Users can freely download relevant data in these databases for conducting research, based on which users can also draft related articles for publication. Our research is based on open-source data from these datasets and follows the data access policies and publication guidelines of these datasets, with no ethical concerns or any conflicts of interest. Therefore, this study was exempted from obtaining approval from the local ethics committee (Zhejiang Center of Laboratory Animals) as per the committee's guidelines.

Author Contributions

All authors made a significant contribution to the work reported, whether that is in the conception, study design, execution, acquisition of data, analysis and interpretation, or in all these areas; took part in drafting, revising or critically reviewing the article; gave final approval of the version to be published; have agreed on the journal to which the article has been submitted; and agree to be accountable for all aspects of the work.

Funding

This work was funded by the General Scientific Research Project of Zhejiang Provincial Department of Education (grant number: Y201942728), and Zhejiang Medical and Health Science and Technology Planning Project (grant number: 2021KY523).

Disclosure

The authors declare no competing interests in this work.

References

1. Smyth EC, Nilsson M, Grabsch HI, van Grieken NC, Lordick F. Gastric cancer. *Lancet*. 2020;396(10251):635–648. doi:10.1016/S0140-6736(20)31288-5
2. Kole C, Charalampakis N, Tsakatikas S, et al. Immunotherapy for gastric cancer: a 2021 update. *Immunotherapy*. 2022;14(1):41–64. doi:10.2217/imt-2021-0103
3. Alipour M. Molecular mechanism of helicobacter pylori-induced gastric cancer. *J Gastrointest Cancer*. 2021;52(1):23–30. doi:10.1007/s12029-020-00518-5
4. Maddineni G, Xie JJ, Brahmbhatt B, Mutha P. Diet and carcinogenesis of gastric cancer. *Curr Opin Gastroenterol*. 2022;38(6):588–591. doi:10.1097/MOG.0000000000000875
5. Taja-Chayeb L, Vidal-Millan S, Trejo-Becerril C, et al. Hereditary diffuse gastric cancer (HDGC). An overview. *Clin Res Hepatol Gastroenterol*. 2022;46(4):101820. doi:10.1016/j.clinre.2021.101820
6. Zhang Y, Cong X, Li Z, Xue Y. Estrogen facilitates gastric cancer cell proliferation and invasion through promoting the secretion of interleukin-6 by cancer-associated fibroblasts. *Int Immunopharmacol*. 2020;78:105937. doi:10.1016/j.intimp.2019.105937
7. Huang W, Jiang Y, Xiong W, et al. Noninvasive imaging of the tumor immune microenvironment correlates with response to immunotherapy in gastric cancer. *Nat Commun*. 2022;13(1):5095. doi:10.1038/s41467-022-32816-w
8. Shi T, Zhang Y, Wang Y, et al. DKK1 promotes tumor immune evasion and impedes anti-PD-1 treatment by inducing immunosuppressive macrophages in gastric cancer. *Cancer Immunol Res*. 2022;10(12):1506–1524. doi:10.1158/2326-6066.CIR-22-0218
9. Zhao W, Liu M, Zhang M, et al. Effects of inflammation on the immune microenvironment in gastric cancer. *Front Oncol*. 2021;11:690298. doi:10.3389/fonc.2021.690298
10. Cuzick J, Thorat MA, Bosetti C, et al. Estimates of benefits and harms of prophylactic use of aspirin in the general population. *Ann Oncol*. 2015;26(1):47–57. doi:10.1093/annonc/mdu225
11. Zhao H, Wu L, Yan G, et al. Inflammation and tumor progression: signaling pathways and targeted intervention. *Signal Transduct Target Ther*. 2021;6(1):263. doi:10.1038/s41392-021-00658-5
12. Schaue D, Micewicz ED, Ratikan JA, Xie MW, Cheng G, McBride WH. Radiation and inflammation. *Semin Radiat Oncol*. 2015;25(1):4–10. doi:10.1016/j.semradonc.2014.07.007
13. Vasan N, Baselga J, Hyman DM. A view on drug resistance in cancer. *Nature*. 2019;575(7782):299–309. doi:10.1038/s41586-019-1730-1
14. Hao S, Shou M, Ma J, Shu Y, Yu Y. Correlation analysis of serum pepsinogen, interleukin, and TNF-alpha with hp infection in patients with gastric cancer: a randomized parallel controlled clinical study. *Comput Math Methods Med*. 2022;2022:9277847. doi:10.1155/2022/9277847
15. Davakis S, Kapelouzou A, Sakellariou S, et al. Clinical and oncological impact of the toll-like receptor-3 and −4 in esophageal and gastro-esophageal junction adenocarcinoma. *Anticancer Res*. 2023;43(7):3183–3191. doi:10.21873/anticanres.16492
16. Liu H, Xiang Y, Zong QB, et al. miR-6745-TIMP1 axis inhibits cell growth and metastasis in gastric cancer. *Aging*. 2021;13(21):24402–24416. doi:10.18632/aging.203688
17. Zhou K, Song B, Wei M, Fang J, Xu Y. MiR-145-5p suppresses the proliferation, migration and invasion of gastric cancer epithelial cells via the ANGPT2/NOD_LIKE_RECEPTOR axis. *Cancer Cell Int*. 2020;20(1):416. doi:10.1186/s12935-020-01483-6
18. Liu Y, Wei D, Deguchi Y, et al. PPARdelta dysregulation of CCL20/CCR6 axis promotes gastric adenocarcinoma carcinogenesis by remodeling gastric tumor microenvironment. *Gastric Cancer*. 2023. doi:10.1007/s10120-023-01418-w
19. Chen W, Qin Y, Liu S. CCL20 signaling in the tumor microenvironment. *Adv Exp Med Biol*. 2020;1231:53–65. doi:10.1007/978-3-030-36667-4_6
20. Chen X, Chen R, Jin R, Huang Z. The role of CXCL chemokine family in the development and progression of gastric cancer. *Int J Clin Exp Pathol*. 2020;13(3):484–492.
21. Ma X, Wang N, Chen K, Zhang C. Oncosuppressive role of MicroRNA-205-3p in gastric cancer through inhibition of proliferation and induction of senescence: oncosuppressive role of MicroRNA-205 in gastric cancer. *Transl Oncol*. 2021;14(11):101199. doi:10.1016/j.tranon.2021.101199
22. Cheng X, Fan K, Wang L, et al. Correction: tfR1 binding with H-ferritin nanocarrier achieves prognostic diagnosis and enhances the therapeutic efficacy in clinical gastric cancer. *Cell Death Dis*. 2022;13(11):998. doi:10.1038/s41419-022-05453-w
23. Zhou Z, Xia G, Xiang Z, et al. A C-X-C chemokine receptor type 2-dominated cross-talk between tumor cells and macrophages drives gastric cancer metastasis. *Clin Cancer Res*. 2019;25(11):3317–3328. doi:10.1158/1078-0432.CCR-18-3567

24. Zhang Q, Chai S, Wang W, et al. Macrophages activate mesenchymal stem cells to acquire cancer-associated fibroblast-like features resulting in gastric epithelial cell lesions and malignant transformation in vitro. *Oncol Lett*. 2019;17(1):747–756. doi:10.3892/ol.2018.9703
25. Miao L, Qi J, Zhao Q, et al. Targeting the STING pathway in tumor-associated macrophages regulates innate immune sensing of gastric cancer cells. *Theranostics*. 2020;10(2):498–515. doi:10.7150/thno.37745
26. Rihawi K, Ricci AD, Rizzo A, et al. Tumor-associated macrophages and inflammatory microenvironment in gastric cancer: novel translational implications. *Int J Mol Sci*. 2021;22(8). doi:10.3390/ijms22083805.
27. Corvino D, Kumar A, Bald T. Plasticity of NK cells in Cancer. *Front Immunol*. 2022;13:888313. doi:10.3389/fimmu.2022.888313
28. Stockis J, Roychoudhuri R, Halim TYF. Regulation of regulatory T cells in cancer. *Immunology*. 2019;157(3):219–231. doi:10.1111/imm.13064
29. Shafabakhsh R, Pourhanifeh MH, Mirzaei HR, Sahebkar A, Asemi Z, Mirzaei H. Targeting regulatory T cells by curcumin: a potential for cancer immunotherapy. *Pharmacol Res*. 2019;147:104353. doi:10.1016/j.phrs.2019.104353
30. Wang L, Fu Y, Chu Y. Regulatory B Cells. *Adv Exp Med Biol*. 2020;1254:87–103. doi:10.1007/978-981-15-3532-1_8
31. Jeppsson S, Srinivasan S, Chandrasekharan B. Neuropeptide Y (NPY) promotes inflammation-induced tumorigenesis by enhancing epithelial cell proliferation. *Am J Physiol Gastrointest Liver Physiol*. 2017;312(2):G103–G111. doi:10.1152/ajpgi.00410.2015
32. Itakura T, Peters DM, Fini ME. Glaucomatous MYOC mutations activate the IL-1/NF-kappaB inflammatory stress response and the glaucoma marker SELE in trabecular meshwork cells. *Mol Vis*. 2015;21:1071–1084.
33. Buttari B, Profumo E, Domenici G, et al. Neuropeptide Y induces potent migration of human immature dendritic cells and promotes a Th2 polarization. *FASEB J*. 2014;28(7):3038–3049. doi:10.1096/fj.13-243485
34. Li Y, Chen S, Li Z. Plasma neuropeptide Y (NPY) levels in patients with gastric and colorectal carcinomas. *Zhonghua Zhong Liu Za Zhi*. 1998;20 (3):213–215.
35. Judge SM, Deyhle MR, Neyroud D, et al. MEF2c-dependent downregulation of myocilin mediates cancer-induced muscle wasting and associates with cachexia in patients with cancer. *Cancer Res*. 2020;80(9):1861–1874. doi:10.1158/0008-5472.CAN-19-1558
36. Mao G, Mu Z, Wu D. Exosome-derived miR-2682-5p suppresses cell viability and migration by HDAC1-silence-mediated upregulation of ADH1A in non-small cell lung cancer. *Hum Exp Toxicol*. 2021;40(12_suppl):S318–S330. doi:10.1177/09603271211041997
37. Zahid KR, Yao S, Khan ARR, Raza U, Gou D. mTOR/HDAC1 crosstalk mediated suppression of ADH1A and ALDH2 links alcohol metabolism to hepatocellular carcinoma onset and progression in silico. *Front Oncol*. 2019;9:1000. doi:10.3389/fonc.2019.01000
38. Li Z, Xie J, Fei Y, et al. GDNF family receptor alpha 2 promotes neuroblastoma cell proliferation by interacting with PTEN. *Biochem Biophys Res Commun*. 2019;510(3):339–344. doi:10.1016/j.bbrc.2018.12.169
39. Gu J, Wang D, Zhang J, et al. Corrigendum to "GFRalpha2 prompts cell growth and chemoresistance through down-regulating tumor suppressor gene PTEN via Mir-17-5p in pancreatic cancer" [Cancer Lett. 380 (2) (2016 Oct 1) 434-41]. *Cancer Lett*. 2019;452:270. doi:10.1016/j.canlet.2019.03.031

Journal of Inflammation Research Dovepress

Publish your work in this journal

The Journal of Inflammation Research is an international, peer-reviewed open-access journal that welcomes laboratory and clinical findings on the molecular basis, cell biology and pharmacology of inflammation including original research, reviews, symposium reports, hypothesis formation and commentaries on: acute/chronic inflammation; mediators of inflammation; cellular processes; molecular mechanisms; pharmacology and novel anti-inflammatory drugs; clinical conditions involving inflammation. The manuscript management system is completely online and includes a very quick and fair peer-review system. Visit http://www.dovepress.com/testimonials.php to read real quotes from published authors.

Submit your manuscript here: https://www.dovepress.com/journal-of-inflammation-research-journal